Inorg. Chem. **2003**, *42*, 552–559

From Metallacyclophanes to 1-D Coordination Polymers: Role of Anions in Self-Assembly Processes of Copper(II) and 2,5-Bis(3-pyridyl)-1,3,4-oxadiazole

Miao Du, Xian-He Bu,* Zheng Huang, Shen-Tan Chen, and Ya-Mei Guo

Department of Chemistry, Nankai University, Tianjin 300071, P. R. China

Carmen Diaz and Joan Ribas

Departament de Química Inorgànica, Universitat de Barcelona, Diagonal 647, 08028-Barcelona, Spain

Received July 6, 2002

The reaction of various Cu^{II} salts with 2,5-bis(3-pyridyl)-1,3,4-oxadiazole (**L**) in $CH_3CN–H_2O$ medium affords different complexes, the solid structures of which are controlled *only* by the choice of the counteranions. Reaction of $Cu(ClO_4)_2·6H_2O$ or $Cu(NO_3)_2·3H_2O$ and **L** yields the novel bimetallic macrocyclic complex $[Cu_2\mathbf{L}_2(H_2O)_6](ClO_4)_4(H_2O)_4$ (**1**) [monoclinic, space group $P2_1/m$, $a = 8.745(5)$ Å, $b = 16.179(10)$ Å, $c = 14.930(8)$ Å, $\beta = 93.253(10)°$, $Z = 2$] or $[Cu\mathbf{L}(NO_3)_2]_2(CH_3CN)_2$ (**2**) [triclinic, space group $P\bar{1}$, $a = 7.863(3)$ Å, $b = 8.679(3)$ Å, $c = 13.375(5)$ Å, $\alpha = 74.121(5)°$, $\beta = 78.407(6)°$, $\gamma = 86.307(6)°$, $Z = 1$]. However, with the replacement of Cu^{II} perchlorate or nitrate salts with $CuSO_4·5H_2O$ or $Cu(OAc)_2·H_2O$ in the above reaction, two different one-dimensional (1-D) coordination polymers $\{[Cu_2\mathbf{L}_2(H_2O)_6(SO_4)_2](H_2O)_6\}_n$ (**3**) [triclinic, space group $P\bar{1}$, $a = 7.078(3)$ Å, $b = 11.565(4)$ Å, $c = 12.561(5)$ Å, $\alpha = 109.511(6)°$, $\beta = 105.265(6)°$, $\gamma = 94.042(6)°$, $Z = 1$] or $\{[Cu_2\mathbf{L}(\mu\text{-}OAc)_4]\}_n$ (**4**) [monoclinic, space group $C2/c$, $a = 20.007(7)$ Å, $b = 7.506(2)$ Å, $c = 16.062(5)$ Å, $\beta = 108.912(5)°$, $Z = 4$] were obtained. These results unequivocally indicate that the nature of the counteranions, which play different roles in each complex, is the key factor governing the structural topologies of them. The magnetic properties of these Cu^{II} complexes have been investigated by variable-temperature magnetic susceptibility and magnetization measurements, and the magneto–structural correlation has been analyzed in detail.

Introduction

Self-assembly processes involving metal ions have attracted much attention in the field of supramolecular chemistry and crystal engineering from the viewpoints of the development of novel functional materials with unique electronic, magnetic, catalytic, and optical properties.[1−3] One of the ultimate goals of supramolecular chemistry is to control the structure of the target products with desired properties and functions, which is mainly reliant on spontaneous self-assembly in most earlier studies.[4] To date, of diverse elegant efforts to find the key factors in the approach to the design of metal-based supramolecules, the main rational synthetic strategy has been the use of various spacer ligands as the "building block". So far, a number of discrete and a wide range of infinite frameworks have already been

* To whom correspondence should be addressed. E-mail: buxh@nankai.edu.cn. Fax: +86-22-23502458. Tel: +86-22-23502809.

(1) (a) Lehn, J.-M. *Supramolecular Chemistry*; VCH: Weinheim, Germany, 1995. (b) Robson, R.; Abrahams, B. F.; Batten, S. R.; Gable, R. W.; Hoskins, B. F.; Liu, J. In *Supramolecular Architecture: Synthetic Control in Thin Films and Solids*; Bein, T., Ed.; ACS Symposium Series 499; American Chemical Society: Washington, DC, 1992; p 256. (c) Braga, D.; Grepioni, F.; Desiraju, G. R. *Chem. Rev.* **1998**, *98*, 1375. (d) Hagrman, P. J.; Hagrman, D.; Zubieta, J. *Angew. Chem., Int. Ed.* **1999**, *38*, 2638. (e) Leininger, S.; Olenyuk, B.; Stang, P. J. *Chem. Rev.* **2000**, *100*, 853.

(2) (a) Batten, S. R.; Robson, R. *Angew. Chem., Int. Ed.* **1998**, *37*, 1460. (b) Reineke, T. M.; Eddaoudi, M.; Moler, D.; O'Keeffe, M.; Yaghi, O. M. *J. Am. Chem. Soc.* **2000**, *122*, 4843. (c) Zaworotko, M. J. *Chem. Commun.* **2001**, 1.

(3) (a) Kahn, O. *Molecular Magnetism*; VCH: Weinheim, Germany, 1993. (b) Philip, O.; Stoddart, J. F. *Angew. Chem., Int. Ed. Engl.* **1996**, *35*, 1154. (c) Yaghi, O. M.; Li, H.; David, C.; Richardson, D.; Groy, T. L. *Acc. Chem. Res.* **1998**, *31*, 474. (d) Chui, S. S.-Y.; Lo, S. M.-F.; Chartmant, J. P. H.; Orpen, A. G.; Williams, I. D. *Science* **1999**, *283*, 1148.

(4) (a) Wolff, J. J. *Angew. Chem., Int. Ed. Engl.* **1996**, *35*, 2195. (b) Davis, M. E. *Chem.—Eur. J.* **1997**, *3*, 1745. (c) Caulder, D. L.; Raymond, K. N. *Acc. Chem. Res.* **1999**, *32*, 975. (d) Lalioti, N.; Raptopoulou, C. P.; Terzis, A.; Aliev, A. E.; Gerothanassis, I. P.; Manessi-Zoupa, E.; Perlepes, S. P. *Angew. Chem., Int. Ed.* **2001**, *40*, 3211.

10.1021/ic025851h CCC: $25.00
Published on Web 12/31/2002

generated with simple 4,4′-bipyridyl-based ligands.[5] Although it has also been known that the structural topologies of such metal complexes can be specifically designed according to the selection of the metal ions with different coordination geometry[6] or radius,[7] counteranions with different coordination ability[8] or bulk,[9] solvent,[10] metal/ligand ratio,[11] and even pH condition,[12] the influence of these factors on the self-assembly processes is still less well understood and *systematic* investigations are quite rare.

On the other hand, in contrast to the well-development on linear 4,4′-N-donor bridging ligands, efforts on 3,3′-N-donor species are still unusual.[10c] Meantime, metal-based supramolecular moieties with Cu^{II} center and bridging ligands are relatively rare, comparing with those of Cu^{I}.[5] In our efforts[13] to investigate the control of the self-assembly of an organic/inorganic supramolecular motif, we have reported a novel Cu^{II} diamondoid interpenetrating network with 2,5-bis(4-pyridyl)-1,3,4-oxadiazole that is dependent on the choice of the anions.[13e] As a continuation of our work, we selected a 3,3′-N-donor ligand, 2,5-bis(3-pyridyl)-1,3,4-oxadiazole (**L**), as the organic spacer in connection with structural control of discrete (e.g. molecular box) or divergent coordination networks (e.g. 1-D zigzag chain) upon metal complexation under appropriate conditions. Theoretically, this ligand has potential tendency to generate three typical isomers (two cisoid and one transoid; see Supporting Information) when coordinating to the metal centers, although the coordination chemistry of it has not been explored. To further develop our understanding of construction the metal-based supramolecules, we studied the role of counteranions in complexes formation with **L**. In this contribution, we report the syntheses and crystal structures of a series of Cu^{II} complexes with **L** exhibiting different topologies. In each case, the ligand (**L**), metal ion (Cu^{II}), solvent (CH_3CN-H_2O), and metal/ligand ratio (1:1) are kept constant, and the only varied parameter during these processes is the counteranion (ClO_4^-, NO_3^-, SO_4^{2-}, and OAc^- for complexes **1**−**4**, respectively). The magnetic properties of these polynuclear Cu^{II} systems have also been studied in detail.

Experimental Section

Materials and General Methods. Most of the starting materials and solvents for syntheses were obtained commercially and used as received. The ligand **L** was synthesized according to the literature method.[14] FT-IR spectra (KBr pellets) were taken on a FT-IR 170SX (Nicolet) spectrometer. Carbon, hydrogen, and nitrogen analyses were performed on a Perkin-Elmer 240C analyzer. ESR spectra were recorded on powder samples at X-band frequency with a Bruker 300E automatic spectrometer, varying the temperature between 4 and 300 K (for **4** it was made only at room temperature because the signal was too weak at low temperature).

Magnetic Studies. The variable-temperature magnetic susceptibilities were measured in "Servei de Magnetoquímica (Universitat de Barcelona)" on polycrystalline samples (ca. 30 mg) with a Quantum Design MPMS SQUID susceptometer operating at a magnetic field of 0.1 T between 2 and 300 K. The diamagnetic corrections were evaluated from Pascal's constants for all the constituent atoms. Magnetization measurements were carried out at low temperature (2 K) in 0−5 T range.

Syntheses of Cu^{II} Complexes. $[Cu_2L_2(H_2O)_6](ClO_4)_4(H_2O)_4$ (1). A solution of $Cu(ClO_4)_2\cdot 6H_2O$ (130 mg, 0.35 mmol) in H_2O (20 mL) was added to a solution of **L** (81 mg, 0.35 mmol) in CH_3CN (10 mL). After ca. 30 min of vigorous mixing, some light blue precipitates were formed and then dissolved in excessive H_2O (40 mL). The resultant solution was filtered and left to stand at room temperature. Block blue single crystals suitable for X-ray analysis were obtained by slow evaporation of the solvent within 1 week. Yield: 50%. Anal. Found: C, 24.73; H, 3.28; N, 9.95. Calcd for $C_{24}H_{36}Cl_4Cu_2N_8O_{28}$: C, 24.99; H, 3.15; N, 9.72. IR (KBr, cm^{-1}): ν 3425 b, 3122 m, 1611 vs, 1559 m, 1487 m, 1419 s, 1343 m, 1283 w, 1143 vs, 1120 vs, 1187 vs, 998 m, 940 m, 815 m, 734 m, 687 s, 734 s, 636 s, 626 vs.

$[CuL(NO_3)_2]_2(CH_3CN)_2$ (2). The same synthetic procedure as for **1** was used except that the $Cu(ClO_4)_2\cdot 6H_2O$ was replaced by $Cu(NO_3)_2\cdot 3H_2O$, giving dark-blue crystals in 70% yield. Anal. Found: C, 37.01; H, 2.59; N, 21.37. Calcd for $C_{28}H_{22}Cu_2N_{14}O_{14}$: C, 37.13; H, 2.45; N, 21.66. IR (KBr, cm^{-1}): ν 2290 w, 2256 m, 1617 s, 1559 m, 1506 s, 1488 vs, 1419 s, 1345 m, 1303 s, 1271 s, 1194 m, 1131 m, 1109 m, 1054 m, 1015 s, 999 s, 831 m, 806 m, 748 w, 733 m, 698 m.

$\{[Cu_2L_2(H_2O)_6(SO_4)_2](H_2O)_6\}_n$ (3). The same synthetic procedure as for **1** was used except that $Cu(ClO_4)_2\cdot 6H_2O$ was replaced by $CuSO_4\cdot 5H_2O$, giving light bluish-green single crystals in 60% yield. It should be noted that the well-shaped crystals of complex **3** were sensitive when exposed to air for a long time and the structure was determined in a sealed capillary. Anal. Found: C, 29.04; H, 4.38; N, 11.66. Calcd for $C_{24}H_{40}Cu_2N_8O_{22}S_2$: C, 29.30; H, 4.10; N, 11.39. IR (KBr, cm^{-1}): ν 3387 b, 1618 s, 1564 m,

(5) (a) Fujita, M.; Ogura, K. *Coord. Chem. Rev.* **1996**, *148*, 249. (b) Fujita, M. *Chem. Soc. Rev.* **1998**, *27*, 417. (c) Stang, P. J.; Zhdankin, V. V. *Chem. Rev.* **1996**, *96*, 1123. (d) Blake, A. J.; Champness, N. R.; Hubberstey, P.; Li, W.-S.; Withersby, A.; Schröder, M. *Coord. Chem. Rev.* **1999**, *183*, 117.

(6) Ma, J. F.; Liu, J. F.; Yan, X.; Jia, H. Q.; Lin, Y. H. *J. Chem. Soc., Dalton Trans.* **2000**, 2403.

(7) (a) Hong, M. C.; Zhao, Y. J.; Su, W. P.; Cao, R.; Fujita, M.; Zhou, Z. Y.; Chan, A. S. C. *Angew. Chem., Int. Ed.* **2000**, *39*, 2468. (b) Hong, M. C.; Zhao, Y. J.; Su, W. P.; Cao, R.; Fujita, M.; Zhou, Z. Y.; Chan, A. S. C. *J. Am. Chem. Soc.* **2000**, *122*, 4819.

(8) Withersby, M. A.; Blake, A. J.; Champness, N. R.; Hubberstey, P.; Li, W.-S.; Schröder, M. *Angew. Chem., Int. Ed. Engl.* **1997**, *36*, 2327.

(9) Carlucci, L.; Ciani, G.; Macchi, P.; Proserpio, D. M.; Rizzato, S. *Chem.—Eur. J.* **1999**, *5*, 237.

(10) (a) Lu, J.; Paliwala, T.; Lim, S. C.; Yu, C.; Niu, T.; Jacobson, A. J. *Inorg. Chem.* **1997**, *36*, 923. (b) Jung, O.-S.; Park, S. H.; Kim, K. M.; Jang, H. G. *Inorg. Chem.* **1998**, *37*, 5781. (c) Withersby, M. A.; Blake, A. J.; Champness, N. R.; Cooke, P. A.; Hubberstey, P.; Li, W.-S.; Schröder, M. *Inorg. Chem.* **1999**, *38*, 2259 and references therein.

(11) (a) Blake, A. J.; Brooks, N. R.; Champness, N. R.; Cooke, P. A.; Deveson, A. M.; Fenske, D.; Hubberstey, P.; Li, W.-S.; Schröder, M. *J. Chem. Soc., Dalton Trans.* **1999**, 2103. (b) Saalfrank, R. W.; Bernt, I.; Chowdhry, M. M.; Hampel, F.; Vaughan, G. B. M. *Chem.—Eur. J.* **2001**, *7*, 2765. (c) Du, M.; Chen, X. T.; Bu, X. H. *Cryst. Growth Des.* **2002**, *2*, 625.

(12) (a) Pan, L.; Huang, X. Y.; Li, J.; Wu, Y. G.; Zheng, N. W. *Angew. Chem., Int. Ed.* **2000**, *39*, 527. (b) Matsumoto, N.; Motoda, Y.; Matsuo, T.; Nakashima, T.; Re, N.; Dahan, F.; Tuchagues, J.-P. *Inorg. Chem.* **1999**, *38*, 1165 and references therein. (c) Du, M.; Bu, X. H.; Guo, Y. M.; Ribas, J.; Diaz, C. *Chem. Commun.* **2002**, 2550.

(13) (a) Bu, X. H.; Biradha, K.; Yamaguchi, T.; Nishimura, M.; Ito, T.; Tanaka, K.; Shionoya, M. *Chem. Commun.* **2000**, 1953. (b) Bu, X. H.; Chen, W.; Lu, S. L.; Zhang, R. H.; Liao, D. Z.; Shionoya, M.; Brisse, F.; Ribas, J. *Angew. Chem., Int. Ed.* **2001**, *40*, 3201. (c) Bu, X. H.; Chen, W.; Du, M.; Zhang, R. H. *Cryst. Eng. Commun.* **2001**, *30*, 1. (d) Bu, X. H.; Chen, W.; Du, M.; Biradha, K.; Wang, W. Z.; Zhang, R. H. *Inorg. Chem.* **2002**, *41*, 437. (e) Bu, X. H.; Chen, W.; Hou, W. F.; Du, M.; Zhang, R. H.; Brisse, F. *Inorg. Chem.* **2002**, *41*, 3477. (f) Du, M.; Bu, X. H.; Guo, Y. M.; Liu, H.; Batten, S. R.; Ribas, J.; Mak, T. C. W. *Inorg. Chem.* **2002**, *41*, 4904.

(14) Bentiss, F.; Lagrenee, M. *J. Heterocycl. Chem.* **1999**, *36*, 1029.

Table 1. Crystal Data and Structure Refinement Parameters for Complexes **1**−**4**

	1	**2**	**3**	**4**
chem formula	$C_{24}H_{36}Cl_4Cu_2N_8O_{28}$	$C_{28}H_{22}Cu_2N_{14}O_{14}$	$C_{24}H_{40}Cu_2N_8O_{22}S_2$	$C_{20}H_{20}Cu_2N_4O_9$
fw	1153.49	905.68	983.84	587.48
cryst syst	monoclinic	triclinic	triclinic	monoclinic
space group	$P2_1/m$	$P\bar{1}$	$P\bar{1}$	$C2/c$
T (K)	293(2)	293(2)	293(2)	293(2)
a (Å)	8.745(5)	7.863(3)	7.078(3)	20.007(7)
b (Å)	16.179(10)	8.679(3)	11.565(4)	7.506(2)
c (Å)	14.930(8)	13.375(5)	12.561(5)	16.062(5)
α (deg)	90	74.121(5)	109.511(6)	90
β (deg)	93.253(10)	78.407(6)	105.265(6)	108.912(5)
γ (deg)	90	86.307(6)	94.042(6)	90
V (Å^3)	2109(2)	859.9(5)	920.7(6)	2282.0(13)
Z	2	1	1	4
ρ_{calcd} (g/cm^3)	1.816	1.749	1.774	1.710
μ (cm^{-1})	13.69	13.29	13.68	19.24
R[a]	0.0604	0.0453	0.0454	0.0342
R_w[b]	0.1302	0.0805	0.1060	0.0854

[a] $R = \sum||F_o| - |F_c||/\sum|F_o|$. [b] $R_w = [\sum[w(F_o^2 - F_c^2)^2]/\sum w(F_o^2)^2]^{1/2}$.

1487 m, 1421 s, 1341 m, 1290 m, 1136 s, 1091 vs, 1051 vs, 1032 s, 986 m, 968 m, 938 w, 824 s, 735 m, 687 s, 657 m, 620 s.

{[Cu$_2$L(μ-OAc)$_4$]}$_n$ (4). The same synthetic procedure as for **1** was used except that the $Cu(ClO_4)_2 \cdot 6H_2O$ was replaced by $Cu(OAc)_2 \cdot H_2O$, giving dark bluish-green single crystals in 85% yield. Anal. Found: C, 41.11; H, 3.29; N, 9.50. Calcd for $C_{20}H_{20}Cu_2N_4O_9$: C, 40.89; H, 3.43; N, 9.54. IR (KBr, cm^{-1}): ν 1614 vs, 1542 m, 1466 s, 1433 vs, 1345 m, 1282 m, 1197 s, 1078 m, 1050 m, 965 w, 816 m, 700 s, 682 s, 642 m, 625 m.

Caution: *Although no problem was encountered in this study, transition metal perchlorate complexes are potentially explosive and should be handled with proper precautions!*

X-ray Data Collection and Structure Determinations. Single-crystal X-ray diffraction studies of complexes **1**−**4** were performed on a Bruker Smart 1000 CCD diffractometer equipped with a graphite crystal monochromator situated in the incident beam for data collection. The determination of unit cell parameters and data collections were performed with Mo Kα radiation (λ = 0.71073 Å) by ω scan mode in the range of $2.77 < \theta < 25.03°$ (for **1**), $1.61 < \theta < 25.03°$ (for **2**), $2.09 < \theta < 25.03°$ (for **3**), and $2.15 < \theta < 25.03°$ (for **4**). The program SAINT[15] was used for integration of the diffraction profiles. All the structures were solved by direct methods using the SHELXS program of the SHELXTL package and refined with SHELXL (semiempirical absorption corrections were applied using the SADABS program).[16] Cu^{II} atoms in each complex were located from the *E*-maps, and other non-hydrogen atoms were located in successive difference Fourier syntheses. The structure of **1** contains disordered perchlorate anions and water molecules. The final refinement was performed by full-matrix least-squares methods with anisotropic thermal parameters for all the non-hydrogen atoms on F^2. The hydrogen atoms of **L** were generated theoretically onto the specific atoms and refined isotropically with fixed thermal factors (the hydrogen atoms of CH_3CN molecule in **2** and coordiantion water molecules in **3** were determined using difference Fourier method). Further details for structural analysis are summarized in Table 1.

Results and Discussion

Synthesis and General Characterization. Compounds **1**−**4** were prepared by the reaction of corresponding Cu^{II} salt and equimolar neutral dipyridyl ligand **L** under almost the same conditions except the counteranions. Complexes **1**−**3** have 1:1 ligand/metal composition, and for **4**, a 1:2 ligand/metal moiety was achieved although all the four complexes were prepared using 1:1 ligand/metal molar ratio. Indeed, **4** can be isolated using 1:1, 1:2, and even 1:5 ligand/metal reaction stoichiometries in CH_3CN-H_2O medium, which was also confirmed by X-ray diffraction (all three products have the same unit cell parameters), IR spectra, and elemental analyses, indicating this reaction is independent to the ligand/metal condition.

In the IR spectra of complexes **1** and **3**, the broad band centered at ca. 3400 cm^{-1} indicates the O−H stretching of the aqua molecules, and the characteristic absorption band with medium intensity of CH_3CN (ν_{CN}) in complex **2** appears at 2256 cm^{-1}. The absorption bands resulting from the skeletal vibrations of aromatic rings for all the four complexes appear in the 1400−1600 cm^{-1} region. For **1**, the occurrence of split ν_{Cl-O} stretches of the ClO_4^- anions at ~1100 cm^{-1} provides good evidence of their involvement in the formation of hydrogen bonding. For **2**, the characteristic bands of the NO_3^- anions appear at 1488 cm^{-1} for $\nu_a(NO_2)$ with very strong intensity, 1303 cm^{-1} for $\nu_s(NO_2)$, and 1015 cm^{-1} for ν(NO). The $\nu_a - \nu_s$ value is 185 cm^{-1}, suggesting the bis-dentate chelated feature of the NO_3^- anions when coordinating to the Cu^{II} center. For **3**, the bands of SO_4^{2-} groups appear at 1032−1136, 968, and 687 cm^{-1}, indicating the monodendate coordination mode (C_{3v} symmetry). The IR spectrum for **4** displays the characteristic bands of the acetate anions at 1614 cm^{-1} for $\nu_{as(C-O)}$, 1433 cm^{-1} for $\nu_{sym(C-O)}$, and 700 cm^{-1} for δ_{O-C-O}. The Δ value ($\nu_{as} - \nu_{sym}$) indicates that the acetate anions coordinate to the Cu^{II} center in bridging mode, which is consistent with the crystal structure as described below.

X-ray Single-Crystal Structures. Bimetallic Macrocycles [Cu$_2$L$_2$(H$_2$O)$_6$](ClO$_4$)$_4$(H$_2$O)$_4$ (1) and [CuL(NO$_3$)$_2$]$_2$·(CH$_3$CN)$_2$ (2). The structure of **1** contains a $[Cu_2L_2(H_2O)_6]^{2+}$ dinuclear cation, in which two **L**'s are related by a mirror plane located through two crystallographically independent Cu^{II} atoms (Figure 1a), ClO_4^- anions, and H_2O molecules.

(15) *SAINT Software Reference Manual*; Bruker AXS: Madison, WI, 1998.
(16) Sheldrick, G. M. *SHELXTL NT Version 5.1. Program for Solution and Refinement of Crystal Structures*; University of: Göttingen: Göttingen, Germany, 1997.

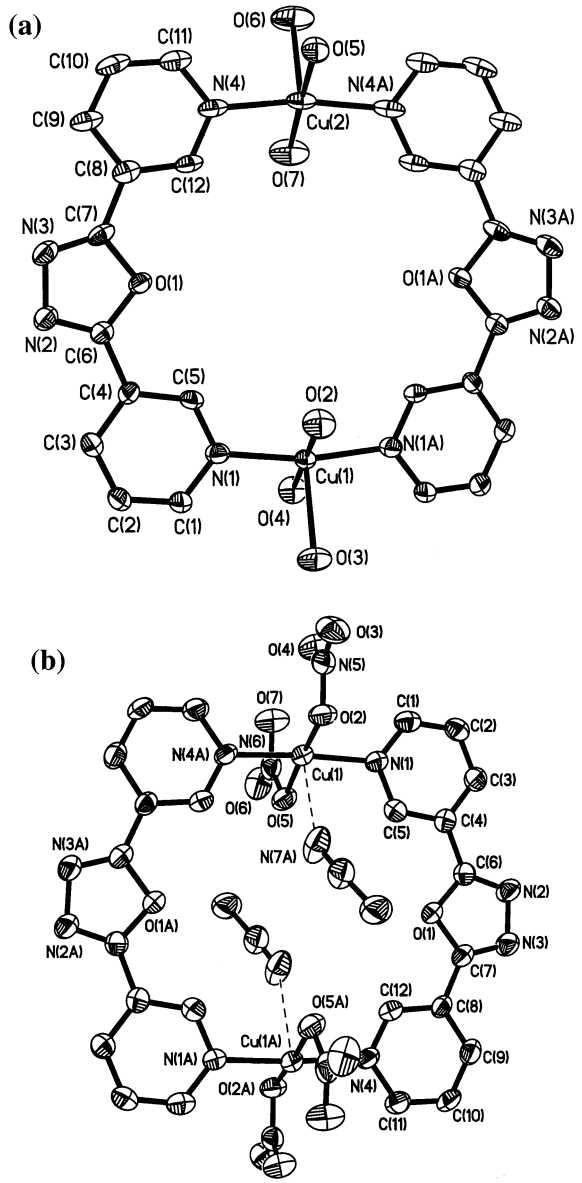

Figure 1. ORTEP structures of (a) $[Cu_2\mathbf{L}_2(H_2O)_6]^{2+}$ cation in **1** and (b) $[Cu\mathbf{L}(NO_3)_2]_2(CH_3CN)_2$ (**2**) with 50% thermal ellipsoid probability.

Both Cu^{II} centers are pentacoordinated to two N atoms of **L** and two O donors of H_2O, forming the basal plane, and one H_2O from axis, taking the distorted square-pyramid geometry with τ parameters of 0.18 for Cu(1) and 0.10 for Cu(2).[17] Cu(1) is 0.109 Å above the basal plane toward apical O(3), and Cu(2) is 0.121 Å toward O(6). The axial elongated Cu−O length is significantly longer than those in basal plane (Table 2). Two ClO_4^- ions locate above and below the macrocycle cation (ca. 7.9 × 7.3 Å^2) with weak Cu−O interactions (Cu(1)−O(21), 2.559 Å; Cu(2)−O(31), 2.683 Å). The nearest intermolecular distances for Cu(1)···Cu(1)^i ($i = x \pm 1, -y, -z$) and Cu(1)···Cu(2)^i ($i = x - 1, y, z$) are 8.745 and 7.985 Å.

The structure of **2** consists of a bimetallic ring $[Cu\mathbf{L}(NO_3)_2]_2$ with a crystallographic center of symmetry and two CH_3CN's. The Cu^{II} center is bound to two N atoms of **L** and two O donors of NO_3^- to form a square-planar geometry (Figure 1b). Two CH_3CN solvents locate above and below

Table 2. Selected Bond Distances (Å) and Angles (deg) for Complex **1**[a]

Cu(1)−O(2)	1.979(6)	Cu(1)−O(4)	1.987(5)
Cu(1)−N(1)	1.999(5)	Cu(1)−O(3)	2.281(6)
Cu(2)−O(7)	1.990(6)	Cu(2)−O(5)	1.999(5)
Cu(2)−N(4)	2.011(6)	Cu(2)−O(6)	2.235(6)
O(2)−Cu(1)−O(4)	179.0(3)	O(2)−Cu(1)−N(1)	88.70(13)
O(4)−Cu(1)−N(1)	91.20(13)	N(1)−Cu(1)−N(1)^i	168.3(3)
O(2)−Cu(1)−O(3)	92.5(3)	O(4)−Cu(1)−O(3)	88.5(2)
N(1)−Cu(1)−O(3)	95.76(13)	O(7)−Cu(2)−O(5)	175.9(3)
O(7)−Cu(2)−N(4)	88.21(13)	O(5)−Cu(2)−N(4)	91.45(13)
N(4)−Cu(2)−N(4)^i	169.7(2)	O(7)−Cu(2)−O(6)	94.2(3)
O(5)−Cu(2)−O(6)	89.9(3)	O(6)−Cu(2)−N(4)	94.93(13)

[a] Symmetry operation: (i) $x, -y + 3/2, z$.

Table 3. Selected Bond Distances (Å) and Angles (deg) for Complex **2**[a]

Cu(1)−N(1)	2.025(3)	Cu(1)−N(4)^i	2.021(3)
Cu(1)−O(2)	1.972(3)	Cu(1)−O(5)	1.984(3)
Cu(1)−N(7)^{ii}	2.592(3)		
O(2)−Cu(1)−O(5)	174.87(13)	O(2)−Cu(1)−N(4)^i	90.22(12)
O(5)−Cu(1)−N(4)^i	89.60(12)	O(2)−Cu(1)−N(1)	93.14(13)
O(5)−Cu(1)−N(1)	86.83(13)	N(1)−Cu(1)−N(4)^i	175.76(14)
O(2)−Cu(1)−N(7)	86.25(12)	O(5)−Cu(1)−N(7)	88.71(13)
N(1)−Cu(1)−N(7)	88.04(13)	N(4)^i−Cu(1)−N(7)	89.77(12)

[a] Symmetry operation: (i) $-x, -y + 2, -z + 2$; (ii) $x, y, z + 1$.

the neutral ring (ca. 7.6 × 7.4 Å^2) with weak Cu−N coordination (2.592(3) Å). Thus, according to the structural data (Table 3), the coordination sphere of Cu^{II} could also be described as a square pyramid ($\tau = 0.015$). Cu(1) is 0.066 Å above the mean basal plane N(1)−N(4A)−O(2)−O(5) toward apical N(7A). The positions of the NO_3^- anions around Cu^{II} are somewhat crowded: there exist several weak interactions such as Cu(1)−O(4) (2.727 Å), Cu(1)−O(7) (2.553 Å), Cu(1)−N(5) (2.746 Å), and Cu(1)−N(6) (2.658 Å), being consistent with the IR spectrum. The nearest intermolecular Cu···Cu^i ($i = -x + 1, -y + 2, -z + 1$) distance is 7.376 Å.

Since the pioneering studies by Fujita[18] and Saalfrank[19] et al. on metallamacrocycles, considerable efforts have been focused on designing such compounds.[1e,4c,20] Complexes **1** and **2** described here are rare water-soluble Cu^{II} metallamacrocycles.[21] Another interesting point is the stacking patterns of the two assembly species in the solid state: (i) For **1**, the cation parts are parallel stacked along *a* axis about 8.0 Å apart to form a column, and the adjacent columns further interlace, resulting in a quasi 3-D-like arrangement (Figure 2a). The closest approach between the interlaced aromatic rings is 3.61 Å. The ClO_4^- and H_2O guests in the cavities link each other and the cations through hydrogen bonds, which may further stabilize this structure. (ii) For **2**, one intermolecular C(2)−H(2A)···O(7)^i ($i = -x + 1, -y + 2, -z + 1$) hydrogen bond links the neighboring $[Cu\mathbf{L}(NO_3)_2]_2$

(17) (a) Addison, A. W.; Rao, T. N.; Reedijk, J.; van Rijn, J.; Verschoor, G. C. *J. Chem. Soc., Dalton Trans.* **1984**, 1349. (b) O'Sullivan, C.; Murphy, G.; Murphy, B.; Hathaway, B. *J. Chem. Soc., Dalton Trans.* **1999**, 1835.
(18) Fujita, M.; Yakaki, J.; Ogura, K. *J. Am. Chem. Soc.* **1990**, *112*, 5645.
(19) Saalfrank, R. W.; Stark, A.; Peters, K.; von Schnering, H. G. *Angew. Chem., Int. Ed. Engl.* **1988**, *27*, 851.
(20) Stang, P. J.; Olenyuk, B. *Acc. Chem. Res.* **1997**, *30*, 502.
(21) Du, M.; Guo, Y. M.; Bu, X. H.; Ribas, J.; Monfort, M. *New J. Chem.* **2002**, *26*, 645.

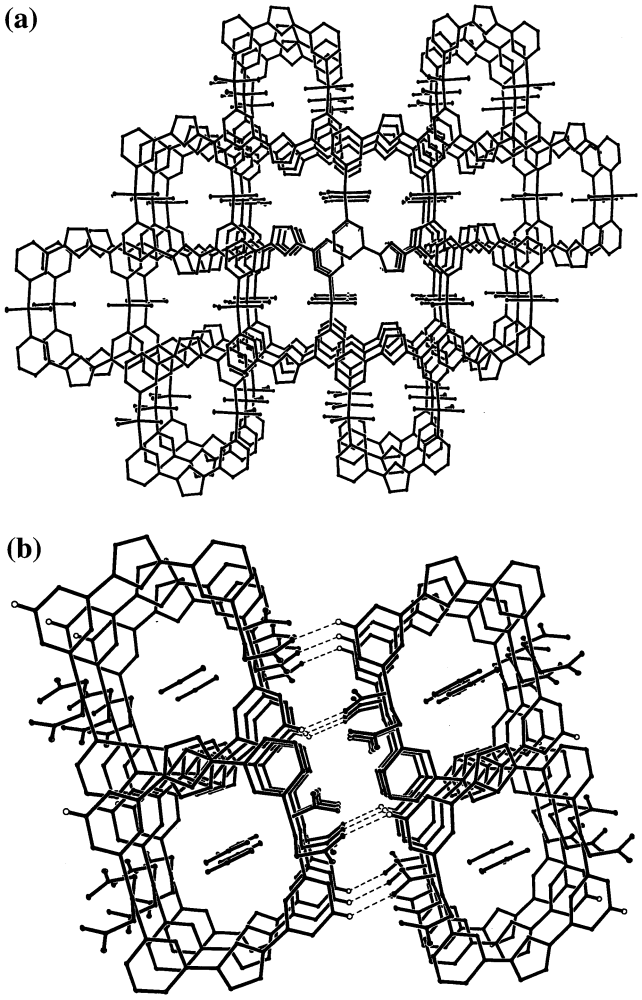

Figure 2. Stacking diagram of (a) **1** and (b) **2** in the unit cell showing the channellike cavities along the *a* direction.

molecules to form a 1-D framework along the *c* direction. These chains also have interlaced 3-D stacking along *a* direction with CH_3CN guests in the cavities (Figure 2b). The separation of the parallel aromatic rings is only 3.35 Å, indicating strong $\pi-\pi$ interactions which stabilize the structure. The interesting zeolite-like arrangements in **1** and **2** may find application in solid-state catalysis, especially in cases where the exact dimensions of the absorbing channels are of importance.[20]

One-Dimensional Coordination Polymers $\{[Cu_2L_2(H_2O)_6(SO_4)_2](H_2O)_6\}_n$ (3) and $\{[Cu_2L(\mu\text{-}OAc)_4]\}_n$ (4). The structure of complex **3** has a neutral 1-D infinite alternate chain motif, in which the Cu^{II} ions are bridged by cisoid-I type ligands **L**. As shown in Figure S1 (see Supporting Information), in the asymmetric dinuclear $[Cu_2L_2(H_2O)_6(SO_4)_2]$ unit, there are two independent octahedral Cu^{II} centers with different coordination environments. Cu(1) is coordinated to two ligands **L** and four aqua molecules, showing considerable Jahn−Teller distortion (see Table 4), with the axial Cu(1)−O(3) distance (2.379(4) Å) elongated in comparison to the two independent Cu(1)−N(4) and Cu(1)−O(2) equatorial distances (2.018(4) and 1.994(3) Å, respectively). However, for the six-coordinated octahedral Cu(2) atom, the elongate axial positions are occupied by the

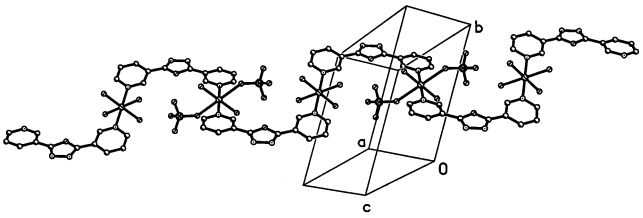

Figure 3. Wavelike one-dimensional framework for complex **3**.

Table 4. Selected Bond Distances (Å) and Angles (deg) for Complex **3**[a]

Cu(1)−O(2)	1.994(3)	Cu(1)−N(4)	2.018(4)
Cu(1)−O(3)	2.379(4)	Cu(2)−N(1)	2.030(4)
Cu(2)−O(4)	1.951(3)	Cu(2)−O(5)	2.478(3)
O(2)−Cu(1)−N(4)^{i}	88.11(15)	O(2)−Cu(1)−N(4)	91.89(14)
O(2)−Cu(1)−O(3)^{i}	87.82(14)	O(2)−Cu(1)−O(3)	92.18(14)
N(4)−Cu(1)−O(3)^{i}	87.01(14)	N(4)−Cu(1)−O(3)	92.99(14)
O(4)−Cu(2)−N(1)	88.33(15)	N(4)−Cu(2)−N(1)^{ii}	91.67(15)
O(5)−Cu(2)−N(1)	92.95(15)	O(5)−Cu(2)−N(1)^{ii}	87.12(15)
O(5)−Cu(2)−O(4)	87.14(15)	O(5)−Cu(2)−O(4)^{ii}	92.90(15)

[a] Symmetry operations: (i) $-x+3, -y+1, -z+1$; (ii) $-x+1, -y+1, -z$.

Table 5. Selected Bond Distances (Å) and Angles (deg) for Complex **4**[a]

Cu(1)−O(14)	1.961(3)	Cu(1)−O(12)^{i}	1.965(2)
Cu(1)−O(13)^{i}	1.969(2)	Cu(1)−O(11)	1.971(2)
Cu(1)−N(1)	2.200(3)	Cu(1)−Cu(1)^{i}	2.617(2)
O(14)−Cu(1)−O(12)^{i}	88.71(12)	O(14)−Cu(1)−O(13)^{i}	168.51(10)
O(12)^{i}−Cu(1)−O(13)^{i}	90.85(11)	O(14)−Cu(1)−O(11)	89.21(12)
O(12)^{i}−Cu(1)−O(11)	168.50(10)	O(13)^{i}−Cu(1)−O(11)	88.94(11)
O(14)−Cu(1)−N(1)	99.89(11)	N(1)−Cu(1)−O(12)^{i}	94.06(10)
N(1)−Cu(1)−O(13)^{i}	91.59(10)	O(11)−Cu(1)−N(1)	97.44(10)

[a] Symmetry operations: (i) $-x+1/2, -y+1/2, -z+1$.

SO_4^{2-} anions with Cu−O bond distance of 2.478(3) Å, significantly longer than those of two independent Cu(2)−N(1) and Cu(2)−O(4) lengths (2.030(4) and 1.951(3) Å, respectively) in the equatorial plane. As shown in Figure 3, the ligands bridge the Cu^{II} centers in trans-arrangement to form a wavelike 1-D structure. In this 1:1 ligand/metal polymeric chain, the neighboring Cu(1)···Cu(2) separation is 8.133 Å and the shortest Cu···Cu distance between the adjacent chains is 7.078 Å.

X-ray single-crystal structure determination reveals that complex **4** is a neutral 1-D coordination polymer with each unit containing a $[Cu_2(OAc)_4]$ dinuclear entity linked by the ligand **L**. Each dinuclear unit results from the pairing of two independent mononuclear Cu^{II} fragments related by a crystallographic center of symmetry as shown in Figure S2. The two Cu^{II} centers are bridged equivalently by four acetate anions in syn−syn mode. Each Cu^{II} atom is bound to five donor atoms (CuO_4N) occupying the vertexes of a perfect square pyramid due to the symmetry of the structure with τ value of zero. Important structural data of **4** are listed in Table 5. Four oxygen atoms of the bridging acetate comprise the basal plane with equivalent Cu−O distances (mean value: 1.967 Å), and the axial coordination site is occupied by one nitrogen donor of the bridging ligand **L** with Cu(1)−N(1) bond length of 2.200(3) Å, which links the $[Cu_2(OAc)_4]$ units to form this chain structure as depicted in Figure 4. Each Cu^{II} ion deviates from the mean equatorial plane of

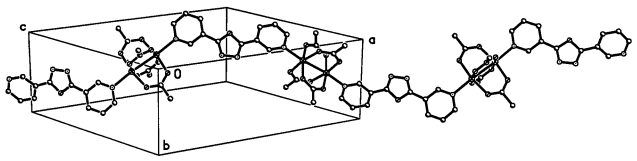

Figure 4. One-dimensional chain construction for compound **4**.

Table 6. Comparison of the Structural Parameters of the Ligand **L** in Complexes **1**−**4**

	1	**2**	**3**	**4**
conformation of **L**	cisoid-I	cisoid-I	cisoid-I	cisoid-II
arrangements of **L**	cis	cis	trans	trans
N−**L**−N (deg)[a]	106.8	105.5	107.9	173.2
Cu−**L**−Cu (deg)[b]	79.2	76.2	81.1	161.0
ϕ (deg)[c]	12.6 and 11.8	7.8 and 2.6	4.8 and 14.3	19.8
θ (deg)[d]	8.2	9.2	17.8	33.6

[a] The angle between the central oxadiazole ring and two N donors of the 3-pyridine. [b] The angle between the central oxadiazole ring and two Cu^{II} centers bridged by the ligand. [c] The dihedral angles between the oxadiazole ring and two 3-pyridine rings. [d] The dihedral angle between the two 3-pyridine rings.

the square pyramid toward the apical nitrogen donor by ca. 0.196 Å. The Cu···Cu distance in the $[Cu_2(OAc)_4]$ unit is only 2.617(2) Å, which is rather short and might suggest some cluster character in this structure. The nonbonding separation of two Cu^{II} centers linked by the ligand **L** in neighboring binuclear units is 12.653 Å, and the shortest Cu···Cu distance between the adjacent chains is 6.650 Å.

It should be interesting and essential to compare the related structural data of the ligand **L** in these Cu^{II} complexes. As listed in Table 6, the ligand **L** adopts the cisoid-I form in complexes **1**−**3** and cisoid-II isomeric form in **4**. As indicated earlier, **L** could generate two cisoid and one transoid isomers when coordinated to the metal centers, at least theoretically. Although **L** has only been observed in the cisoid form in this study,[22] both cisoid and transoid forms have been reported previously for other 3,3′-N-donor bridging ligands, such as 3,6-bis(imidazole-1-yl)pyridazine and 3,3′-dicyanodiphenylacetylene, and it is interesting that the conformations of these ligands observed in the metal complexes appear to be anion-dependent.[23] In complexes **1** and **2**, the ligands surrounding the Cu^{II} centers are in cis arrangement to form the novel metallamacrocyclic architectures. In complexes **3** and **4**, the ligands bridge the Cu^{II} atoms or $[Cu_2(OAc)_4]$ units in trans arrangement to form the 1-D wavelike structures, although **L** takes different conformations in the two complexes. We can see that if the ligands in **3** were in cis arrangement (the other related structural data in **3** are similar to those in **1** and **2**), a similar bimetallamacrocycle structure like **1** and **2** could also be obtained. In complex **4**, the ligand adopts conformation different from those in **1**−**3** and exhibits considerable flexibility when it forms this 1-D structure, which is reflected by the larger values of the dihedral angles between these aromatic rings as listed in Table 6. The change

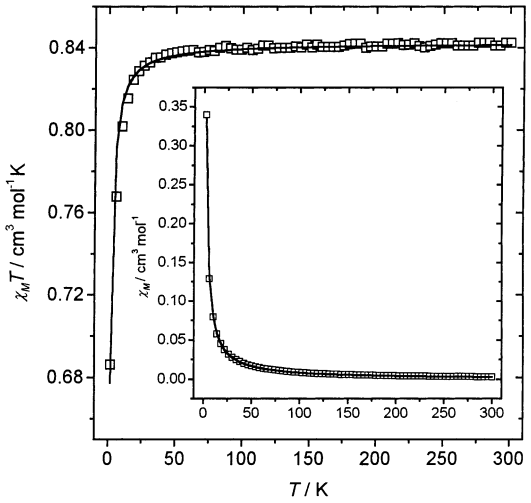

Figure 5. Temperature dependence on $\chi_m T$ or χ_m (insert) for **1**. The solid line represents the best fit (see text for the simulated parameters).

in the conformation and arrangement of the ligands can also be considered as a factor that gives rise to these different structures.

Role of Anions in the Self-assembly Processes. From above descriptions, the choice of anions is clearly critical in determining the molecular structures of the resultant complexes. In this study, the nature (coordinating ability, size, and donor character) of the anions is the underlying reason behind the differences in the structure of this series of Cu^{II} complexes. In complex **1**, ClO_4^- acts as the counteranions to balance the charge and also form hydrogen bonds with the aqua molecules. For **2**, the NO_3^- anions coordinate to the central Cu^{II} atoms and link the molecular rings to form a 1-D structure as donors through intermolecular C−H···O interactions. For **3**, the SO_4^{2-} anions coordinate to one of the Cu^{II} center in the asymmetric dinuclear unit in the 1-D coordination zigzag chain. As indicated above, it seems that this structure is resulted from the trans arrangement of the ligands. However, the large bulk of the SO_4^{2-} anion is the prime reason because it cannot be clathrated in an imaginary bimetallamacrocycle host due to the steric effect. For **4**, four OAc^- groups bridge the Cu^{II} centers to form a $[Cu_2(OAc)_4]$ unit in syn−syn mode, and **L** link these units (from axial position of each Cu^{II} atom) in cisoid-II conformation and trans arrangement due to the steric requirement to form this 1-D linear structure. Thus, direct coordination to metal centers is not the only role of the anions, and indeed extremely subtle templating effects to change the conformation and arrangement of the ligands have also been observed in this study.

Magnetic Properties. The similar magnetic behaviors of **1** and **2** in the form of $\chi_m T$ and χ_m (insert) versus T plots (χ_m is the molar magnetic susceptibility for two Cu^{II} ions) are shown in Figure 5 and Figure S3, respectively. The values of $\chi_m T$ at 300 K are 0.84 cm^3 mol^{-1} K for **1** and 0.92 cm^3 mol^{-1} K for **2**, corresponding to two magnetically quasi-isolated spin doublets. The $\chi_m T$ values smoothly decrease from rt (room temperature) to 50 K and then quickly decrease to 0.68 cm^3 mol^{-1} K for **1** and 0.83 cm^3 mol^{-1} K for **2** at 2 K. These global features are characteristic of very weak

(22) During the review of this manuscript, we obtained a Zn^{II} complex with **L** in which the ligand takes the transoid conformation.

(23) (a) Begley, M. J.; Hubberstey, P.; Stroud, J. *J. Chem. Soc., Dalton Trans.* **1996**, 4295. (b) Hirsch, K. A.; Wilson, S. R.; Moore, J. S. *Inorg. Chem.* **1997**, *36*, 2960.

antiferromagnetic intramolecular (and/or intermolecular) interactions. The χ_m curves are less indicative: they start at 0.0028 $cm^3\ mol^{-1}$ for **1** and 0.003 $cm^3\ mol^{-1}$ for **2** at rt and increase in a uniform way to 0.34 $cm^3\ mol^{-1}$ for **1** and 0.41 $cm^3\ mol^{-1}$ for **2** at 2 K, respectively.

The fit of the $\chi_m T$ data assuming a dinuclear Cu^{II} complex applying the Bleaney−Bowers formula[24] ($H = -J_i \Sigma S_i S_j$) was made. The best-fit parameters are the following: for **1**, $J = -0.96 \pm 0.02\ cm^{-1}$, $g = 2.12$, $R = 1.3 \times 10^{-5}$; for **2**, $J = -0.52 \pm 0.02\ cm^{-1}$, $g = 2.22$, $R = 1.2 \times 10^{-6}$ (R is the agreement factor defined as $\Sigma_i[(\chi_m T)_{obs} - (\chi_m T)_{calc}]^2/\Sigma_i[(\chi_m T)_{obs}]^2$). The J values indicate that the couplings between the intermolecular Cu^{II} centers are very slightly antiferromagnetic (also may be due to the intermolecular interactions between the Cu^{II} dimeric units), in agreement with the long bridging ligand, which does not creates any significant magnetic pathway. The reduced molar magnetization ($M/N\beta$) per Cu_2 entity (Figures S5 and S6) tends to 1.7 electrons for **1** and 1.8 electrons for **2**. This feature also agrees to the very small antiferromagnetic coupling in both complexes.

The magnetic properties of the 1-D complex **3** in the form of $\chi_m T$ and χ_m (insert) versus T plots (χ_m is the molar magnetic susceptibility for one Cu^{II} ion) are shown in Figure S4. The value of $\chi_m T$ at 300 K is 0.474 $cm^3\ mol^{-1}$ K, corresponding to one magnetically quasi-isolated spin doublet. The $\chi_m T$ value smoothly decreases from rt to 50 K and then quickly decreases to 0.395 $cm^3\ mol^{-1}$ K at 2 K. The global feature is characteristic of very weak antiferromagnetic intramolecular (and/or intermolecular) interactions. The χ_m curve is less indicative: it starts at 0.0012 $cm^3\ mol^{-1}$ at rt and increases in an uniform way to 0.20 $cm^3\ mol^{-1}$ at 2 K.

As described in the crystallographic part, **3** exhibits a 1-D chain structure in which the Cu^{II} centers are linked only by the organic bridging ligand **L**. With these considerations, the fit of the $\chi_m T$ data assuming a uniform 1-D Cu^{II} complex applying the reported formula[25] for this kind of system, with the Hamiltonian $H = -J_i \Sigma S_i S_j$, was made. The best-fit parameters are the following: $J = -0.49 \pm 0.02\ cm^{-1}$; $g = 2.20$; $R = 1.6 \times 10^{-6}$ (R is defined as above). The J value indicates that the coupling between the adjacent Cu^{II} centers within one chain is very slightly antiferromagnetic, in agreement with the long bridging ligand, which does not creates any significant magnetic pathway, as stated above. This small antiferromagnetic coupling may also arise from the intermolecular interactions between the chains. The reduced molar magnetization ($M/N\beta$) per Cu^{II} entity tends to 1.0 electron following the Brillouin formula but for a g value lower than that obtained for the fit of susceptibility measurements and ESR spectra (see below), such as in **1** and **2**. This feature also agrees to the very small antiferromagnetic coupling within the Cu^{II} ions.

The magnetic properties of complex **4** in the form of $\chi_m T$ and χ_m versus T plots (χ_m is the molar magnetic susceptibility for two Cu^{II} ions) are shown in Figure 6. The value of $\chi_m T$ at 300 K is 0.57 $cm^3\ mol^{-1}$ K, which is much more smaller than that expected for two magnetically quasi-isolated spin doublets (ca. 0.8 $cm^3\ mol^{-1}$ K). The $\chi_m T$ value decreases from rt to 75 K and then shows a plateau close to nearly zero (0.0064 $cm^3\ mol^{-1}$ K). This feature is characteristic of very strong antiferromagnetic coupling. The χ_m curve is also very much indicative: it starts at 0.0019 $cm^3\ mol^{-1}$ at room temperature, attains a maximum of 0.00203 $cm^3\ mol^{-1}$ between 220 and 200 K, decreases to a minimum of 0.0018 $cm^3\ mol^{-1}$ at 45 K, and then increases to 0.0032 $cm^3\ mol^{-1}$ at 2 K. This feature is clearly indicative of strong antiferromagnetic coupling with some extent of paramagnetic impurities, shown at very low temperatures. These impurities are usually exhibited when the antiferromagnetic coupling is very strong.[24b]

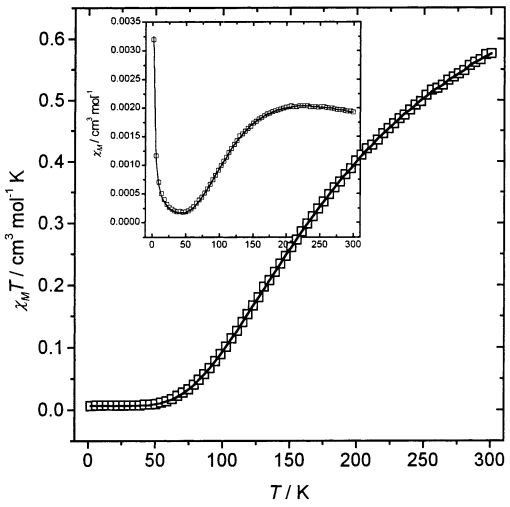

Figure 6. Temperature dependence on $\chi_m T$ or χ_m (insert) for **4**. The solid line represents the best fit (see text for the simulated parameters).

To analyze the magnetic properties of this 1-D complex, it is interesting to divide the structure in two parts: the dinuclear $[Cu_2(OAc)_4]$ moiety and the ligand **L** which bridges these dinuclear entities. As shown in complexes **1**−**3**, the coupling through the bridging ligand **L** is very small when **L** is directed toward the $d_{x^2-y^2}$ magnetic orbital (with the unpaired electron of Cu^{II}); thus, when **L** is directed toward the basal-apical position such as in this complex, the coupling must be zero. That is, the main characteristic of **4** from the view of magnetism is the dinuclear $[Cu_2(OAc)_4]$ building blocks and there are no coordination polymers with all the metal centers communicating. Therefore, the magnetic behavior of **4** is not unexpectedly special. Then, we can assume that it is simply a dinuclear Cu^{II} complex from the point of magnetism, and the fit of the $\chi_m T$ data applying again the Bleaney−Bowers formula,[24] with the Hamiltonian $H = -J_i \Sigma S_i S_j$, was made. The best-fit parameters are the following: $J = -254.5 \pm 2\ cm^{-1}$; $g = 2.22$; ρ (paramagnetic impurities) = 1.4%; $R = 1.3 \times 10^{-5}$ (R is defined as above). This J value indicates that the coupling between the Cu^{II} centers is very strongly antiferromagnetic, in agreement with the existence of four syn−syn carboxylato groups (it should be noted that as indicated in other systems with strong antiferromagnetic coupling,[26] when the diamagnetic correc-

(24) (a) Bleaney, B.; Bowers, K. D. *Proc. R. Soc. London, Ser. A.* **1952**, *214*, 451. (b) Kahn, O. *Molecular Magnetism;* VCH: Weinheim, Germany, 1993.
(25) Estes, W. E.; Gavel, D. P.; Hatfield, W. E.; Hogdson, D. *Inorg. Chem.* **1978**, *17*, 1415.

tion is of the same order of the magnitude as that of the uncorrected molar susceptibility, the uncertainty of the corrected χ_m values is large, affording estimated J values reliable only within 90−95%). The reduced molar magnetization ($M/N\beta$) per Cu_2 entity tends to 0.03 electrons (see Supporting Information), and this feature also agrees with the very strong antiferromagnetic coupling within the two Cu^{II} ions (the expected value would be close to 2 at 5 T).

To interpret this J value, let us comment that the carboxylato group is one of the most widely used bridging ligands for designing polynuclear complexes with interesting magnetic properties. Its versatility as a ligand is illustrated by the variety of its coordination modes when acting as a bridge,[27] the most common being the so-called syn−syn, syn−anti, and anti−anti modes. For Cu^{II} complexes, the former conformation usually mediates a large antiferromagnetic interaction (singlet−triplet energy gap ≈ -350 cm^{-1}).[28] Recently, an interesting theoretical study has been made by Rodriguez-Fortea et al.,[29] illustrating that the syn−syn acetate bridging groups create a very strong antiferromagnetic coupling when there are four carboxylato groups. When the coordination sphere of Cu^{II} is square-pyramid without deviation to trigonal bipyramid (the Cu^{II} atoms in complex **4** is in perfect square-pyramid arrangement as indicated above), the antiferromagnetic coupling is very strong (in such complexes with four bridges, there is a varying degree of out-of-plane displacement of the Cu^{II} atoms from the basal plane of the square-pyramid). Rodriguez-Fortea et al. has demonstrated that the absolute value of the coupling constant increases as the Cu^{II} atoms are separated, regardless of the axial ligands. In **4**, the Cu···Cu distance is 2.617 Å, and for this distance, the theoretical calculation gives a J value of -284 cm^{-1}, which is consistent with the experimental result.

EPR Spectra. For complexes **1**−**3**, the X-band EPR polycrystalline powder spectra show the typical signal for Cu^{II} centers corresponding to the $\Delta M_s = \pm 1$ followed transition (≈3200 G), with no significant variation from room temperature to 4 K, which is consistent with the very weak antiferromagnetic coupling between the Cu^{II} centers in these complexes as indicated above. The following EPR parameters were obtained in these three cases: $g_{\|} = 2.30$; $g_{\perp} = 2.10$; $\langle g \rangle = 2.17$ for **1**; $g_{\|} = 2.28$; $g_{\perp} = 2.11$, $\langle g \rangle = 2.17$ for **2**; $g_{\|} = 2.30$; $g_{\perp} = 2.08$; $\langle g \rangle = 2.16$ for **3**. They have the relationship $g_{\|} > g_{\perp} > 2.00$. The EPR spectrum for **4** shows, as expected, a completely different pattern: at rt there is the typical spectrum for an $S = 1$ state (Figure 7), which corresponds to the higher energy state in the acetate-bridged complex **4** (assuming a dinuclear unit, as made in the susceptibility measurement). The best simulation EPR spectrum of **4** is also given in Figure 7, and the corresponding parameters are the following: $g_x = g_y = 2.10$; $g_z = 2.31$; $D = 0.46$ cm^{-1}; $\Delta H_{x,y} = 500$ G; $\Delta H_z = 300$ G. The value of the main parameter (D) agrees with those reported in the literatures for the EPR spectra of such $[Cu_2(OAc)_4]$ complexes with similar J values.[30]

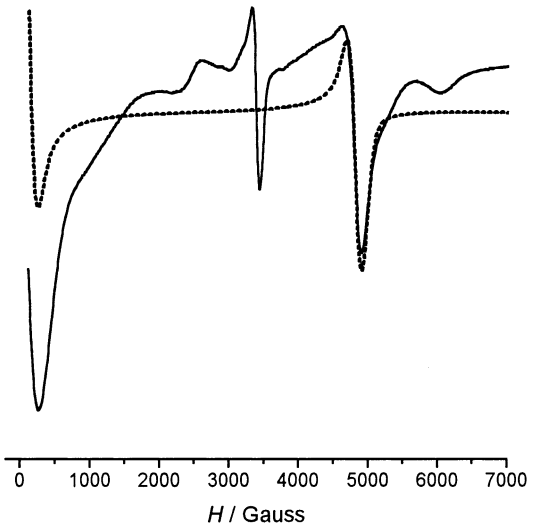

Figure 7. EPR spectrum at room temperature for complex **4** (solid line). The best simulation is shown as a dotted line (see text for the simulated parameters). The central part of the experimental EPR spectrum (at H close to 3000 G) corresponds to the paramagnetic impurities of mononuclear Cu^{II} and is not simulated.

Conclusion and Comments

A series of Cu^{II} complexes with a 3,3′-N-donor bridging ligand 2,5-bis(3-pyridyl)-1,3,4-oxadiazole (**L**) have been synthesized in CH_3CN-H_2O medium and structurally characterized by X-ray diffraction analyses. The molecular structures of these Cu^{II} complexes are profoundly influenced by the anions: bimetallic macrocyclic structures with different dimensional arrangements or 1-D coordination chains with different bridges are observed. This study clearly indicates the important role that the coordination ability/mode and/or bulk of the counteranions can play in crystal engineering and suggests that, given the simple permutations of the anions, Cu^{II} ion alone might also have a rich and diverse role in framework chemistry. Further studies of the self-assemblies of **L** with other metal ions under various conditions are under way in our laboratory.

Acknowledgment. This work was financially supported by National Science Foundation of China (Grant No. 29971019) and the Spanish government (Grant BQU2000-0791).

Supporting Information Available: Four X-ray crystallographic files in CIF format for **1**−**4**, figures showing coordination geometries of Cu^{II} for **3** and **4**, X-band EPR polycrystalline powder spectra for **1**−**3** at 4 K, magnetic diagrams for **2** and **3**, and magnetization measurements for **1**−**4**. This material is available free of charge via the Internet at http://pubs.acs.org.

IC025851H

(26) Akhriff, Y.; Server-Carrió, J.; Sancho, A.; García-Lozano, J.; Escrivá, E.; Folgado, J. V.; Soto, L. *Inorg. Chem*. **1999**, *38*, 1174.
(27) (a) Deacon, G. B.; Phillips, R. J. *Coord. Chem. Rev.* **1980**, *33*, 227. (b) Melnik, M. *Coord. Chem. Rev.* **1981,** *36*, 1. (c) Kato, M.; Muto, Y. *Coord. Chem. Rev.* **1988**, *92*, 45.
(28) (a) Figgis, B. N.; Martin, R. L. *J. Chem. Soc.* **1956**, 3837. (b) Doedens, R. J. *Prog. Inorg. Chem*. **1990**, *38*, 97.
(29) Rodríguez-Fortea, A.; Alemany, P.; Alvarez, S.; Ruiz, E. *Chem.*−*Eur. J*. **2001**, *7*, 627.
(30) (a) Bencini, A.; Gatteschi, D. *EPR of Exchange Coupled Systems*; Springer-Verlag: Berlin, 1989. (b) Muto, Y.; Horie, H.; Tokii, T.; Nakashima, M.; Koikawa, M.; Steward, O. W.; Ohba, S.; Uekusa, H.; Husebye, S.; Suzuki, I.; Kato, M. *Bull. Chem. Soc. Jpn*. **1997**, *70*, 1573 and references therein.